Intramolecular Singlet and Triplet Excimers of Triply Bridged [3.3.*n*](3,6,9)Carbazolophanes

Hiroaki Benten,[†] Jiamo Guo,[†] Hideo Ohkita,*[,†] Shinzaburo Ito,[†] Masahide Yamamoto,[‡] Naoki Sakumoto,[§] Kazushige Hori,[§] Yasuo Tohda,[§] and Keita Tani[§]

Department of Polymer Chemistry, Graduate School of Engineering, Kyoto University, Katsura, Nishikyo, Kyoto 615-8510, Japan, Faculty of Science and Engineering, Ritsumeikan University, Kusatsu, Shiga 525-8577, Japan, and Division of Natural Science, Osaka Kyoiku University, Asahigaoka, Kashiwara, Osaka 582-8582, Japan

Received: March 23, 2007; In Final Form: June 15, 2007

Intermoiety electronic interactions in the singlet and triplet excimer states of triply bridged [3.3.*n*](3,6,9)-carbazolophanes ([3.3.*n*]Cz, $n = 3-6$) were studied by emission and transient absorption measurements. In these [3.3.*n*]Cz molecules, the dihedral angle and the separation distance r between fully overlapped two carbazole rings change systematically from nearly parallel ($n = 3$, $r = 3.35$ Å) to oblique ($n = 6$, $r = 4.03$ Å). In rigid glass at 77 K, [3.3.*n*]Cz ($n = 3$, 4) ($r < 4$ Å) exhibited red-shifted and structureless excimer fluorescence and phosphorescence while [3.3.*n*]Cz ($n = 5$, 6) ($r > 4$ Å) exhibited monomer-like vibrational fluorescence and phosphorescence. In solution at 130 K, all [3.3.*n*]Cz molecules exhibited an excimeric fluorescence band while [3.3.5]Cz still exhibited monomer-like phosphorescence. Transient absorption spectra measured at 294 K exhibited local excitation and charge-transfer bands for all [3.3.*n*]Cz molecules in the excited singlet and triplet states, suggesting that not only singlet but also triplet excimers of carbazole are formed at room temperature. Furthermore, the singlet−triplet energy gap decreased with the decrease in n, suggesting that electrons are effectively delocalized over the two carbazole moieties. These findings showed that both singlet and triplet excimers of carbazole are formed with a separation distance shorter than about 4 Å and are most stable in the parallel-sandwich structure and that the configurational mixing between exciton resonance and charge resonance states plays an essential role in the formation of singlet and triplet excimers of carbazole.

Introduction

Since the first report of the pyrene singlet excimer in solution by Förster and Kasper[1] in 1954, photophysical properties of singlet excimer have been widely reported from both experimental and theoretical viewpoints.[2−9] Historically, various flexible bischromophoric compounds, in which two chromophores are connected with an oligomethylene chain, have been used to investigate the ability of excimer formation, the binding energy, and the preferred geometrical structure in solution.[10−18] Hirayama has studied the formation of excimers for a variety of diphenyl and triphenyl alkanes in solution and found that intramolecular excimers can be formed only when the two phenyl groups are separated by three carbon atoms ($n = 3$ rule).[10] The $n = 3$ rule is widely applicable to other bischromophoric molecules such as dinaphthyl alkanes[11−13] and 1,3-bis(*N*-carbazolyl)propane.[14,15] After studying a series of α,ω-di(1-pyrenyl)alkanes, Zachariasse and Kühnle reported that the most stable excimer is formed at $n = 3$, though excimer fluorescence is observed at other oligomethylene chain lengths as well.[16] These findings suggest that the intramolecular singlet excimer is most stable when the two chromophores can overlap in a symmetric sandwich or totally eclipsed geometry with their short and long in-plane molecular axes essentially parallel. On the other hand, another singlet excimer called the partially overlapped excimer has been found to be formed in polymers having chromophores besides the more stable fully overlapped excimer.[19−28] From a study of excimer formation in sterically hindered poly(3,6-di-*tert*-butyl-9-vinylcarbazole) and its dimeric model compounds, Ito et al. revealed that the carbazole singlet excimer has continuous energy levels depending on the overlapping of carbazole rings.[27,28] Theoretical studies have suggested that two types of resonance interactions play an important role in excimer formation of many aromatic molecules: exciton resonance (ER) and charge resonance (CR) interaction.[2−5] The excimer fluorescence states are considered to be a mixture of the ER and CR states through configurational interaction.[6−9] Theoretically, the interplanar distance in the singlet excimer is estimated to be 3.0−3.6 Å from stabilization energy of the excimer state that is experimentally observed.[7,9]

Compared with these extensive studies on singlet excimers, there are only a few studies on the triplet excimer because of the weak phosphorescence emission in solution. In polymeric systems, the excimer phosphorescence has been observed for some polymers having carbazolyl[29−38] and naphthyl[39,40] groups because of an efficient migration of triplet exciton to a small amount of excimer-forming sites, which work as deep "traps". However, the geometrical structure and the number of chromophores in the excimer-forming sites are still not clear because of the lack of experimental results on excimer phosphorescence from the bischromophoric model compounds in solution. Heretofore, the triplet excimer in solution has been investigated

* To whom correspondence should be addressed. E-mail: ohkita@photo.polym.kyoto-u.ac.jp.
[†] Kyoto University.
[‡] Ritsumeikan University.
[§] Osaka Kyoiku University.

10.1021/jp0723214 CCC: $37.00
Published on Web 08/24/2007

mostly by transient absorption spectroscopy instead of phosphorescence measurements. Zachariasse et al.[41] and Tamai et al.[42] independently observed two different absorption bands for 1,3-di(9-phenanthryl)propane, a monomer-like triplet−triplet $T_n \leftarrow T_1$ absorption band and a new band attributed to the intramolecular triplet excimer of the phenanthryl groups, and concluded that the geometrical structure of this excimer was a fully overlapped sandwich type. On the other hand, Lim et al. studied the naphthalene triplet excimer and proposed that the L-shaped alignment of chromophores is one of the preferred geometries, which is different from the stable geometry in the corresponding singlet excimer.[43−45] They found a new band assigned to the intermoiety charge-transfer (CT) transition in the $T_n \leftarrow T_1$ absorption spectrum and considered this CT band as a criterion of the formation of triplet excimer. These reports demonstrate that the geometrical structure of the triplet excimer still remains controversial.

Cyclophane compounds in which two aromatic rings are fixed in face-to-face orientations by bridging with oligomethylene chains are excellent models for studying the intrachromophoric interactions on the basis of geometrical alignments of the two moieties.[46−68] Thus, photophysical properties of singlet excimers with specific conformation have been elucidated with the aid of various cyclophane compounds (e.g., naphthalenophane,[47,49,52,57] anthracenophane,[51,52] pyrenophane,[50,52] phenanthrenophane,[49,58,60] and carbazolophene[63−66]). Very few cyclophane compounds,[62,63] however, exhibit excimer phosphorescence even in the solid matrices, although the corresponding excimer fluorescence is observed under the same condition. This striking difference indicates that the intermoiety interaction in the triplet state is much weaker than that in the corresponding excited singlet state or that the preferred conformation of triplet excimer is different from a symmetrical sandwich geometry. A recent theoretical study suggested that phosphorescence from the dimer conformation with inversion symmetry is strictly forbidden because of not only electronic spin multiplicity but also spatial orbital symmetry.[44] However, neither the preferred conformation of triplet excimer nor the reason for the difference in the stability between singlet and triplet excimers has been elucidated completely. For these reasons, an experimental study using a series of cyclophane compounds that show an excimer phosphorescence has been desirable to address these unresolved problems. Previously, we investigated the fluorescence and phosphorescence spectra of *syn*- and *anti*-[3.3](3,9)carbazolophanes as model compounds of fully and partially overlapped carbazole excimers, respectively.[63,65] We revealed that *syn*-[3.3]-(3,9)carbazolophane forms triplet excimer in rigid glass at 77 K while *anti*-[3.3](3,9)carbazolophane under the same conditions shows a weak triplet interaction.[63] A recent study of time-resolved electron paramagnetic resonance (EPR) spectroscopy also supported the intermoiety interactions in the triplet states of these carbazolophanes.[68] Hence, we synthesized a series of novel triply bridged [3.3.*n*](3,6,9)carbazolophanes ([3.3.*n*]Cz, $n = 3, 4, 5, 6$) as model compounds for the fully overlapped carbazole excimer to discuss the conformational dependence of the intermoiety interactions in more detail.[67] We have already investigated the ground-state absorption and the fluorescence property of [3.3.*n*]Cz in a solution at room temperature.[66] All [3.3.*n*]Cz molecules exhibited a structureless excimer fluorescence band without any monomer component whose peak is red-shifted with the decrease in bridge length, *n*. Herein, we report on the intermoiety interactions of not only singlet but also triplet excimers and their preferred conformations, which were studied by using the same carbazolophanes [3.3.*n*]Cz ($n = 3, 4, 5$, or 6). These carbazolophanes have unique structures that the dimer configuration varies from a parallel-sandwich to largely inclined depending on the number of methylene units bridging the two carbazole units at their 9-position. In order to clarify the relationship between the excimer interaction and the geometrical structure in the singlet and triplet states, we employed the steady-state emission and the time-resolved transient absorption measurements of the carbazolophanes at several different temperatures: 77 K (rigid glass); 130 and 294 K (liquid solution).

Experimental Section

Materials. 3,6-Dimethyl-*N*-ethylcarbazole (DMeCz) was prepared by the reduction of 3,6-bis(bromomethyl)-*N*-ethylcarbazole with $NaBH_4$. [3.3.*n*](3,6,9)Carbazolophanes ([3.3.*n*]Cz, $n = 3, 4, 5, 6$) were synthesized by intramolecular cyclization of 1,3-bis[3,6-bis(bromomethyl)-*N*-carbazolyl]alkane or 1,3-bis-[3,6-bis(chloromethyl)-*N*-carbazolyl]butane with NH_2CN. Details of the synthesis have been described elsewhere.[67] Solvents used here were benzene (Wako, spectroscopic grade), tetrahydrofuran (THF, Wako, spectroscopic grade), and 2-methyl tetrahydrofuran (MTHF, Tokyo Chemical Industry). Benzene and THF were used without further purification. Prior to use, MTHF was dried with solid KOH, passed through freshly activated alumina, and then distilled from CaH_2 with 2,6-di-*tert*-butyl-*p*-cresol. Poly(butyl methacrylate) (PBMA, Scientific Polymer Products, $M_w = 10 \times 10^4$) was used as a glassy solid matrix after purification by reprecipitation from a benzene solution into methanol, three times.

Methods. Samples dissolved in THF or MTHF were degassed by the freeze−pump−thaw method and sealed in a 1 cm quartz cell. For steady-state absorption and emission measurements and fluorescence decay measurements, the concentration of DMeCz and [3.3.*n*]Cz in the solutions was adjusted to be in the order of 10^{-5} mol L^{-1}. For transient absorption measurements, the concentration of the chromophores in the solutions was 1.3×10^{-4} for [3.3.4]Cz and in the order of 10^{-5} mol L^{-1} for other compounds. A polymer film of PBMA doped with chromophores was prepared on a quartz plate by the solution casting method from benzene solution. The molar concentration of chromophores in the polymer matrix was adjusted to be in the order of 10^{-3} mol L^{-1}.

Steady-state absorption and emission spectra were measured in a 1 cm quartz cell with a spectrophotometer (Hitachi, U-3500) and a fluorescence spectrophotometer (Hitachi, F-4500), respectively. Phosphorescence spectra were collected in a time domain longer than 2 ms after excitation by using a mechanical chopper incorporated in the fluorescence spectrophotometer (Hitachi, F-4500).

Fluorescence decay was measured by the time-correlated single-photon counting (TCSPC) method. The excitation light source was third harmonic pulses (295 nm) generated from a mode-locked Ti:sapphire laser (Spectra Physics, Tsunami 3950) that was pumped with an Ar^+ laser (Spectra Physics, BeamLok 2060). The fluorescence emission was detected with a photomultiplier (PMT, Hamamatsu Photonics, R3234) through a monochromator (Ritsu, MC-10N) with a cutoff filter for the excitation light. The PMT signal was sent to a constant fraction discriminator (Ortec, model 583) and served as the start pulse for a time-to-amplitude converter (TAC, Ortec, model 457). The residual third harmonic pulse was detected with a photodiode (Antel Optronics, AR-32) to provide the stop pulse for the TAC converter through a 100 MHz discriminator (Ortec, model 436). The TAC signal was transferred to a multichannel analyzer

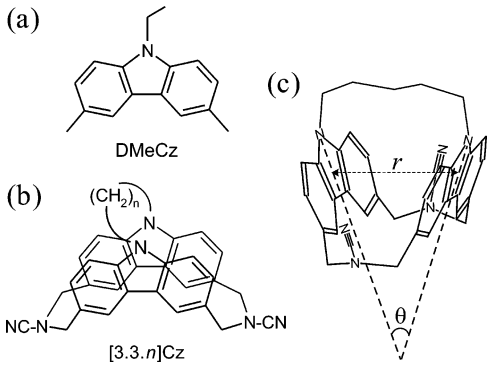

Figure 1. Chemical structure of carbazole compounds: (a) 3,6-dimethyl-*N*-ethylcarbazole (DMeCz), (b) [3.3.*n*](3,6,9)carbazolophane ([3.3.*n*]Cz), (c) mutual orientation of two carbazole moieties in [3.3.*n*]-Cz. The average separation distance *r* and the dihedral angle θ formed between two carbazole rings vary depending on the number of methylene units *n*: $r = 3.35$ Å, $\theta = 2.6°$ ($n = 3$); 3.66 Å, 17.2° ($n = 4$); 4.01 Å, 30.6° ($n = 5$); 4.03 Å, 33.1° ($n = 6$). The average separation distance *r* was calculated by averaging the distances between a pair of atoms in 1- to 9-position in each carbazole ring. Note that the average values of two structures were employed for [3.3.5]Cz because two independent but similar molecular structures were contained in the unit cell.

(Laboratory Equipment Corporation, 2100C/MCA). The total instrument response function has a full width at half-maximum (fwhm) of ca. 750 ps at the excitation wavelength.

Picosecond transient absorption data were measured by the pump and probe method. Third harmonic pulses (355 nm, <2.5 mJ cm^{-2}, 25 ps fwhm) from a Nd:YAG laser (EKSPLA, PL2143) were used as the pump light source. White continuum light generated by focusing the fundamental of the Nd:YAG laser (1064 nm) into a 10 cm D_2O/H_2O (3:1 v/v) quartz cell was used as the probe light source, which was divided into two beams with a half mirror. The probe beam passing through the sample and the other reference beam were independently detected with two multichannel detectors (Hamamatsu Photonics, PMA-11 C7473-37).

Submicrosecond transient absorption measurements were carried out using the same excitation light source as that used for the picosecond measurements. A steady-state 150 W xenon lamp (Hamamatsu Photonics, L2175) was used as a monitor light source. The monitor light in the direction normal to the excitation light passing through the sample was detected with a photomultiplier tube (Hamamatsu Photonics, R5108 or R1477) through a monochromator (Ritsu, MC-10N) for the measurements in the region of 500−1000 nm.

The temperature of the samples sealed in a 1 cm quartz cell was controlled in a heat bath of isopentane. The quartz cell was immersed in a Dewar cell filled with isopentane precooled with liquid nitrogen, and the temperature was measured with a thermocouple. The temperature of the polymer film sample cast on a quartz plate was controlled in a cryostat (Iwatani Plantech, CRT510) with a proportional-integral-derivative (PID) temperature control unit (Scientific Instruments, model 9650).

Results

Structures of [3.3.*n*](3,6,9)Carbazolophanes. The structures of [3.3.*n*]Cz ($n = 3, 4, 5, 6$) compounds have been determined by X-ray analyses.[67] Figure 1 shows the chemical structures of the carbazole compounds used in this study and the mutual orientation of carbazole moieties in [3.3.*n*]Cz. Two carbazole rings completely overlap each other regardless of the number of methylene units *n* bridging the two carbazole moieties at their 9-position. The average separation distance *r* decreases from 4.03 ($n = 6$) to 3.35 Å ($n = 3$), and the dihedral angle θ between the two carbazole rings decreases from 33.1° ($n = 6$) to 2.6° ($n = 3$). In other words, the conformation of the carbazole dimers systematically varies from the largely inclined to parallel-sandwich type in close proximity with decreasing *n*.

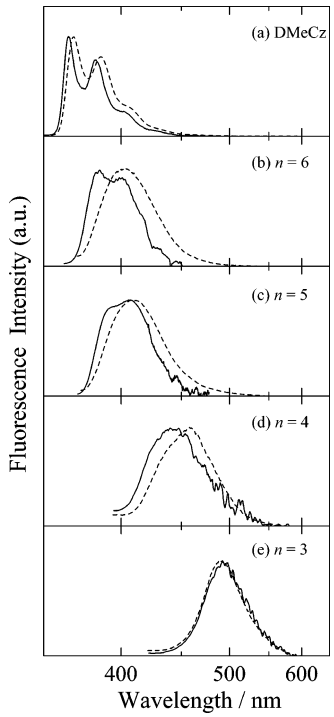

Figure 2. Fluorescence spectra of DMeCz and [3.3.*n*]Cz ($n = 3, 4, 5, 6$) in MTHF rigid glass at 77 K (solid lines) and in solution at 130 K (broken lines): (a) DMeCz, (b) [3.3.6]Cz, (c) [3.3.5]Cz, (d) [3.3.4]Cz, and (e) [3.3.3]Cz. Excitation wavelength was 330 nm. Fluorescence spectra at 77 K were obtained by subtracting the corresponding phosphorescence fraction with a long lifetime from the total emission spectra. Fluorescence intensity was normalized.

Fluorescence Spectra. The solid lines in Figure 2 show fluorescence spectra of DMeCz and [3.3.*n*]Cz ($n = 3, 4, 5, 6$) in MTHF rigid glass at 77 K, which were obtained by subtracting the phosphorescence fraction with a long lifetime from the total emission spectra. The spectral shape systematically varied from weakly structured monomer-like emission to structureless excimer-like emission with decreasing *n*. The [3.3.*n*]Cz ($n = 5, 6$) molecules exhibited rather monomer-like fluorescence with vibrational bands, though they were weakened and shifted to slightly longer wavelengths compared with the 0−0 fluorescence band of DMeCz monomer, while the [3.3.*n*]Cz ($n = 3, 4$) molecules exhibited broad fluorescence largely red-shifted. On the other hand, as shown by the broken lines in Figure 2, all [3.3.*n*]Cz molecules exhibited broad excimer-like fluorescence in the MTHF liquid solution at 130 K, consistent with those at room temperature as already reported.[66] The peak shifts from the 0−0 fluorescence band of DMeCz were as follows: 2397 cm^{-1} ($n = 6$), 2736 cm^{-1} ($n = 5$), 5349 cm^{-1} ($n = 4$), and 6749 cm^{-1} ($n = 3$) in energy (Table 1). These fluorescent species are safely assigned to [3.3.*n*]Cz, and not impurities, because the excitation spectra of the fluorescence component were identical to the corresponding absorption spectra.

Phosphorescence Spectra. Figure 3 shows the ground-state absorption, phosphorescence, and phosphorescence excitation spectra of DMeCz and [3.3.*n*]Cz ($n = 3, 4, 5, 6$) in MTHF rigid glass at 77 K. As shown on the right side of the figure,

TABLE 1: Peak Wavelength λ_{max} and Peak Shift $\Delta\tilde{\nu}$ in Excimer Emission of [3.3.*n*]Cz (n = 3, 4, 5, 6) in MTHF Solution at 130 K

		[3.3.3]Cz	[3.3.4]Cz	[3.3.5]Cz	[3.3.6]Cz
singlet	λ_{max}^{S} (nm)[a]	490	458	409	404
excimer	$\Delta\tilde{\nu}^{S}$ (cm^{-1})[b]	6749	5349	2736	2397
triplet	λ_{max}^{T} (nm)[c]	516	500		
excimer	$\Delta\tilde{\nu}^{T}$ (cm^{-1})[d]	4287	3674		

[a] Peak wavelength of singlet excimer. [b] Peak shift $\Delta\tilde{\nu}^{S}$ was calculated by $\Delta\tilde{\nu}^{S} = \tilde{\nu}_0^{S} - \tilde{\nu}_e^{S}$, where $\tilde{\nu}_0^{S}$ is peak wavenumber of the 0−0 band of DMeCz fluorescence at 368 nm and $\tilde{\nu}_e^{S}$ is peak wavenumber of excimer fluorescence. [c] Peak wavelength of triplet excimer. [d] Peak shift $\Delta\tilde{\nu}^{T}$ was calculated by $\Delta\tilde{\nu}^{T} = \tilde{\nu}_0^{T} - \tilde{\nu}_e^{T}$, where $\tilde{\nu}_0^{T}$ is peak wavenumber of the 0−0 band of DMeCz phosphorescence at 422 nm and $\tilde{\nu}_e^{T}$ is peak wavenumber of excimer phosphorescence.

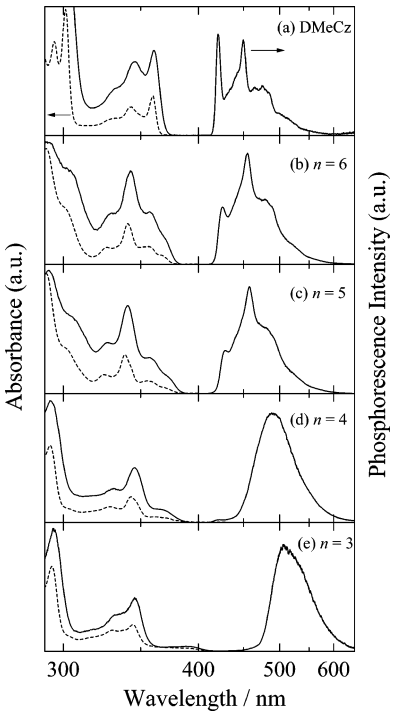

Figure 3. Phosphorescence (solid lines, right), phosphorescence excitation (solid lines, left), and ground-state absorption (broken lines) spectra of DMeCz and [3.3.*n*]Cz (n = 3, 4, 5, 6) in MTHF rigid glass at 77 K: (a) DMeCz, (b) [3.3.6]Cz, (c) [3.3.5]Cz, (d) [3.3.4]Cz, and (e) [3.3.3]Cz. Excitation wavelength was 330 nm. The phosphorescence spectra were normalized. The phosphorescence excitation spectra were measured at 450 nm for DMeCz, 455 nm for [3.3.6]Cz, 457 nm for [3.3.5]Cz, 488 nm for [3.3.4]Cz, and 505 nm for [3.3.3]Cz.

DMeCz monomer exhibited structured emission with characteristic vibrational bands at 420 and 450 nm, which can be assigned to the phosphorescence of the carbazole monomer.[63] On the other hand, the phosphorescence spectra of [3.3.*n*]Cz changed from vibrational to completely broad band with decreasing *n*. As is the case with the fluorescence spectra at 77 K, the [3.3.*n*]Cz (n = 5, 6) molecules exhibited rather monomer-like phosphorescence with vibrational bands at 420 and 450 nm, which are characteristics of the DMeCz monomer, while the [3.3.*n*]Cz (n = 3, 4) molecules exhibited red-shifted and broad phosphorescence. The left side of Figure 3 shows the phosphorescence excitation spectra (solid lines) and the ground-state absorption spectra (broken lines). As shown in this figure, the excitation spectra were identical to the corresponding ground-state absorption spectra. These results clearly show that the phosphorescence observed comes from DMeCz or [3.3.*n*]-Cz molecules and not from impurities. In MTHF solution at 130 K, as seen in Figure 4, the phosphorescence spectra

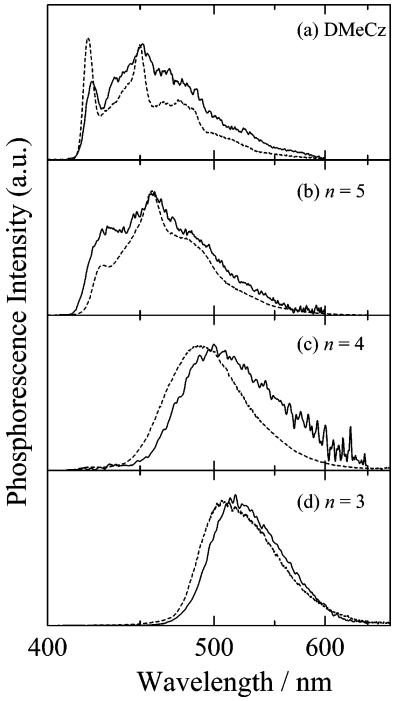

Figure 4. Phosphorescence spectra of DMeCz and [3.3.*n*]Cz (n = 3, 4, 5) in MTHF solution at 130 K (solid lines) and in MTHF rigid glass at 77 K (broken lines): (a) DMeCz, (b) [3.3.5]Cz, (c) [3.3.4]Cz, and (d) [3.3.3]Cz. Excitation wavelength was 330 nm. The phosphorescence intensity was normalized.

essentially remained the same as those observed at 77 K, though they were slightly broadened or red-shifted. The [3.3.5]Cz molecule still had the vibrational structure in the phosphorescence spectrum whereas [3.3.*n*]Cz (n = 3, 4) exhibited a slightly red-shifted broad phosphorescence similar to that at 77 K. The peak shift from the 0−0 band of the monomer phosphorescence was 3674 cm^{-1} for [3.3.4]Cz and 4287 cm^{-1} for [3.3.3]Cz in energy, as summarized in Table 1. Note that the phosphorescence intensity decreased drastically because of thermal deactivation enhanced by intramolecular vibrations in the liquid phase. Consequently, the phosphorescence of [3.3.6]Cz could not be detected at 130 K with our spectrophotometer. Figure 5 shows the total emission spectrum of [3.3.5]Cz in PBMA film at 77 K. The dashed-dotted line represents the phosphorescence spectrum at the same temperature. The broken line was obtained from the subtraction of the phosphorescence spectrum from the total emission; it represents the fluorescence spectrum. The [3.3.5]Cz molecules exhibited broad excimer-like fluorescence and vibrational monomer-like phosphorescence in the PBMA glassy film at 77 K, which are different from that obtained in MTHF at 77 K. The difference will be discussed in detail later.

Transient Absorption Spectra. Figure 6 shows the transient absorption spectra at 50 ps after the laser excitation of DMeCz and [3.3.*n*]Cz (n = 3, 4, 5, 6) in degassed THF solution at 294 K. The DMeCz molecule exhibited two absorption bands at 635 and 790 nm. The 635 nm band is ascribed to $S_n \leftarrow S_1$ absorption of the carbazole monomer, consistent with previous reports.[69] The 790 nm band can be ascribed to carbazole radical cation[70] because it decayed faster than the 635 nm band and the yield was highly suppressed in nonpolar solutions or under low excitation intensity condition. On the other hand, all [3.3.*n*]Cz molecules exhibited two distinct absorption bands in the visible and near-IR range. The visible absorption band was observed at around 695 nm for all [3.3.*n*]Cz molecules regardless of the number *n*. However, the near-IR band was blue-shifted from 1080 to 850 nm with decreasing *n* (Table 2). There was no

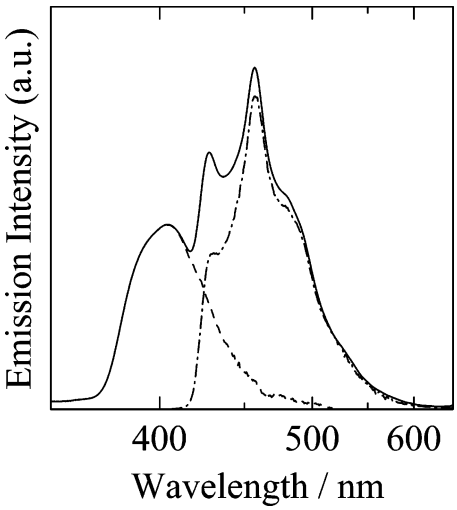

Figure 5. Total emission spectrum of [3.3.5]Cz in PBMA film at 77 K (solid line). The broken and dashed-dotted lines represent the fluorescence and phosphorescence fractions, respectively. The fluorescence fraction was obtained by subtracting the corresponding phosphorescence fraction with a long lifetime from the total emission. Excitation wavelength was 330 nm.

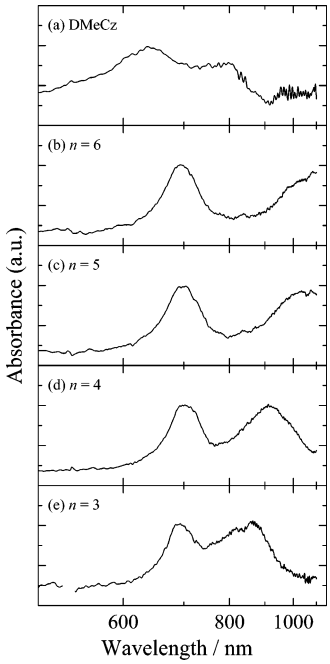

Figure 6. $S_n \leftarrow S_1$ transient absorption spectra of DMeCz and [3.3.*n*]-Cz ($n = 3, 4, 5, 6$) in THF at 294 K at 50 ps after the laser excitation: (a) DMeCz, (b) [3.3.6]Cz, (c) [3.3.5]Cz, (d) [3.3.4]Cz, and (e) [3.3.3]-Cz. The absorbance was normalized.

TABLE 2: Peak Wavelength of the CT Band λ_{CT} in Transient Absorption Spectra of [3.3.*n*]Cz ($n = 3, 4, 5, 6$) in THF Solution at 294 K

	[3.3.3]Cz	[3.3.4]Cz	[3.3.5]Cz	[3.3.6]Cz
λ_{CT}^{S} (nm)[a]	850	918	1055	1080
λ_{CT}^{T} (nm)[b]	690	720	800	800

[a] Peak wavelength of the CT band in $S_n \leftarrow S_1$ transient absorption spectra. [b] Peak wavelength of the CT band in $T_n \leftarrow T_1$ transient absorption spectra.

spectral change from the laser excitation for a few nanoseconds. As shown in Figure 7, no rise component was observed and the absorption bands just decayed monoexponentially with the same lifetime as those of the corresponding excimer fluorescence

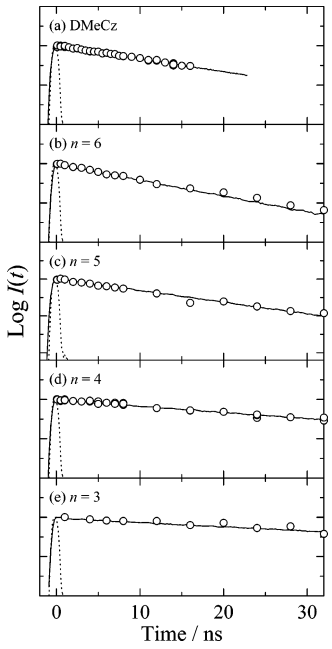

Figure 7. Transient absorption decays of [3.3.*n*]Cz in THF solution at 294 K (open circles). Monitor wavelengths were 635 nm (DMeCz), 850 nm ($n = 3$), 920 nm ($n = 4$), 1050 nm ($n = 5$), and 1080 nm ($n = 6$). The solid lines represent fluorescence decays of [3.3.*n*]Cz in MTHF solution at 294 K and the dotted lines are the instrument response function for the TCSPC measurement.[66]

of each [3.3.*n*]Cz under the same condition. This agreement proves that these absorption bands are ascribed to the fluorescence state in each [3.3.*n*]Cz. We assigned the 695 nm band to a local excitation (LE) band of the excimer state and the near-IR band to a CT band owing to the intermoiety interaction, as we discuss in detail below.

We also studied the transient absorption of DMeCz and [3.3.*n*]Cz ($n = 3, 4, 5, 6$) at 294 K on a longer time scale beyond microsecond to address electronic interactions between carbazole moieties in the phosphorescence states. As shown in Figure 8a, DMeCz exhibited an absorption band around 570 nm assigned to $T_n \leftarrow T_1$ absorption of the carbazole monomer.[71] On the other hand, all the carbazolophanes had two absorption bands, one around 620 nm and the other at a longer wavelength. As with the transient absorption spectra at 50 ps, the 620 nm band was observed for all [3.3.*n*]Cz molecules regardless of *n* while the other band was blue-shifted with decreasing *n* (Table 2). These two bands decayed monoexponentially with the same lifetime in each carbazolophane. We therefore assigned the 620 nm band to an LE band and the other band observed at a longer wavelength to a CT band originating from intermoiety interaction. In a separate experiment, the latter band was suppressed for [3.3.5]Cz at 130 K, consistent with our assignment. A more detailed kinetic study will be reported elsewhere.

Discussion

Intermoiety Interaction in the Singlet Excited State. As described above, [3.3.*n*]Cz ($n = 3, 4$) and [3.3.*n*]Cz ($n = 5, 6$) showed different fluorescence spectra at 77 K. In the MTHF rigid glass at 77 K, all the carbazolophanes are considered to be frozen in the most stable conformation, which would be similar to the crystalline structures revealed by the X-ray analysis. The average separation distance *r* between the two carbazole rings is reported to be 3.35 Å for [3.3.3]Cz, 3.66 Å for [3.3.4]Cz, 4.01 Å for [3.3.5]Cz, and 4.03 Å for [3.3.6]Cz.[67] The difference in the fluorescence spectra gives an important

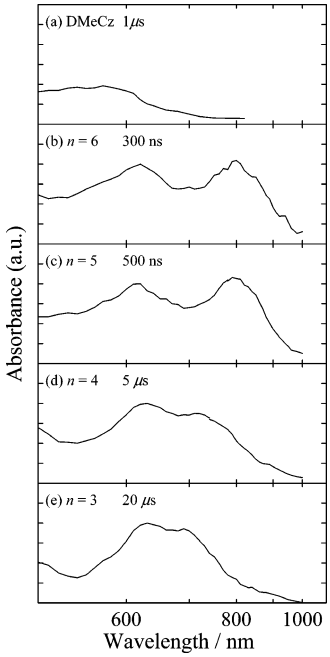

Figure 8. $T_n \leftarrow T_1$ transient absorption spectra of DMeCz and [3.3.*n*]-Cz ($n = 3, 4, 5, 6$) in THF at 294 K: (a) DMeCz, (b) [3.3.6]Cz, (c) [3.3.5]Cz, (d) [3.3.4]Cz, and (e) [3.3.3]Cz. Delay times are indicated in each figure. The absorbance was normalized.

suggestion for the excimer formation in the excited singlet state. We consider $r \sim 4$ Å to be the critical distance for formation of the carbazole singlet excimer. This distance dependence cannot be explained by the ER interaction based on long-range dipole−dipole interaction, indicating that the configurational mixing between the ER and CR states plays a primary role in the formation of the carbazole singlet excimer. The spectral change observed for [3.3.*n*]Cz ($n = 5, 6$) from 77 to 130 K is probably caused by the configurational mixing associated with small conformational relaxation in the excited states. Indeed, the [3.3.*n*]Cz ($n = 5, 6$) molecules exhibited clear excimer fluorescence in PBMA glassy solid even at 77 K, suggesting that the free volume around chromophores may be larger than that in the MTHF glass. According to theoretical calculations for aromatic hydrocarbons, even a small decrease of 0.5 Å in the interplanar separation distances smaller than 3.5−4 Å, where the orbital overlap between chromophores becomes effective and significant, would enhance stabilization by more than 0.4 eV in the fluorescence state.[9] In other words, the intermoiety electronic interaction in the fluorescence state of [3.3.*n*]Cz is strong enough to form a singlet excimer and becomes larger with a decrease in *n*, although the conformational change for the excimer formation in carbazolophanes is so small that we can still discuss the excimer structure on the basis of the ground-state structure.

To address the contribution of the configurational mixing between the ER and CR states to the singlet excimer formation, we employed the pump and probe transient absorption measurements in a picosecond time domain. The absence of $S_n \leftarrow S_1$ absorption of the carbazole monomer or rise component in the transient spectra just after the excitation suggests that the formation of singlet excimer has been almost completed within the laser pulse excitation (~25 ps). The excimer fluorescence without any monomer component and the exciton interaction observed for the ground-state absorption spectra[66] also support the immediate formation of singlet excimer in [3.3.*n*]Cz molecules. Here, we focus on the relaxed excimer state and discuss the energetic scheme of singlet and triplet excimers in [3.3.*n*]Cz on the basis of our spectroscopic data. For various aromatic compounds, the excimer fluorescence state is theoretically considered to be a configurational mixing state of an ER state ($^1\Psi_{ER}$) with a CR state ($^1\Psi_{CR}$) in the same symmetry.[2−4,6−9] The configurational interaction between the two states leads to the excimer fluorescence state ($^1\Psi_{ER-CR}$) lower than the ER state ($^1\Psi_{ER}$) and to another state ($^1\Psi_{ER+CR}$) higher than the CR state ($^1\Psi_{CR}$). Katoh et al. have reported transient absorption spectra for intermolecular singlet excimer of some aromatic molecules and have assigned a characteristic band observed in the near-IR range to a transition from the excimer fluorescence state ($^1\Psi_{ER-CR}$) to a higher state ($^1\Psi_{ER+CR}$) with a CT character.[72] Therefore, the CT band we observed in the transient absorption measurement was also ascribed to a transition from the $^1\Psi_{ER-CR}$ state to the $^1\Psi_{ER+CR}$ state. Figure 9 shows a schematic energy diagram for interaction in carbazole excimers. In this figure, Cz, ^{1}Cz*, and ^{3}Cz* represent the carbazole molecule in the ground state, excited singlet state, and excited triplet state, respectively. The Cz + Cz state represents a pair of carbazole molecules with a large separation distance, where there is no interaction between them. The Cz Cz state represents a pair of carbazole molecules in the dimer configuration, where there is a repulsive interaction between them. Thus, the ^{1}Cz* Cz and ^{3}Cz* Cz states are destabilized by the repulsion energy R_m relative to the ^{1}Cz* + Cz and ^{3}Cz* + Cz states, where the excited state is localized at one Cz moiety. Here, we assumed that the repulsion energy R_m is 0.2 eV on the basis of the theoretical estimation for aromatic hydrocarbons.[7,73] The ^{1}Cz* Cz ↔ Cz ^{1}Cz*, ^{3}Cz* Cz ↔ Cz ^{3}Cz*, and Cz^+ Cz^- ↔ Cz^- Cz^+ states represent the singlet ER state, triplet ER state, and CR state, respectively. The energy level of the CR state in the dimer configuration E(CR) is also assumed to be located by 0.2 eV higher than that of a radical ion pair state ($Cz^+ + Cz^-$). The energy level of the radical ion pair state E(RIP) is approximately estimated by eq 1, because the stabilization energy of the CR interaction Δ is negligible.[3,4]

$$E(\mathrm{RIP}) = \mathrm{IP} - \mathrm{EA} + C(r) \pm \Delta \sim \mathrm{IP} - \mathrm{EA} + C(r) \quad (1)$$

Here IP and EA are the ionization potential and the electron affinity of the monomer, respectively. The Coulomb interaction between the cation and anion $C(r)$ can be estimated by,

$$C(r) = -\frac{e^2}{4\pi\epsilon_0\epsilon r} \quad (2)$$

where e is the elementary charge, ϵ_0 is the vacuum permittivity, ϵ is the dielectric constant of the medium, and r is the separation distance between the cation and anion. The value of IP − EA in polar medium was estimated using eq 3,[72] because it is different from that in vacuum $IP_g - EA_g$ due to the polarization energy induced by the cation and anion $P_\pm$.

$$\mathrm{IP} - \mathrm{EA} = \mathrm{IP_g} - \mathrm{EA_g} + P_+ + P_- \quad (3)$$

The polarization energy P can be estimated by Born's formula,[74]

$$P = P_+ = P_- = \frac{e^2}{8\pi\epsilon_0 R}\left(1 - \frac{1}{\epsilon}\right) \quad (4)$$

where R is the effective radius of the ion. Born's formula has been reported to give reasonable values when the van der Waals radius R_{vdW}[75] is used as the effective radius R of the ion.[76] Therefore, the R_{vdW} of DMeCz was used as R of the ion.

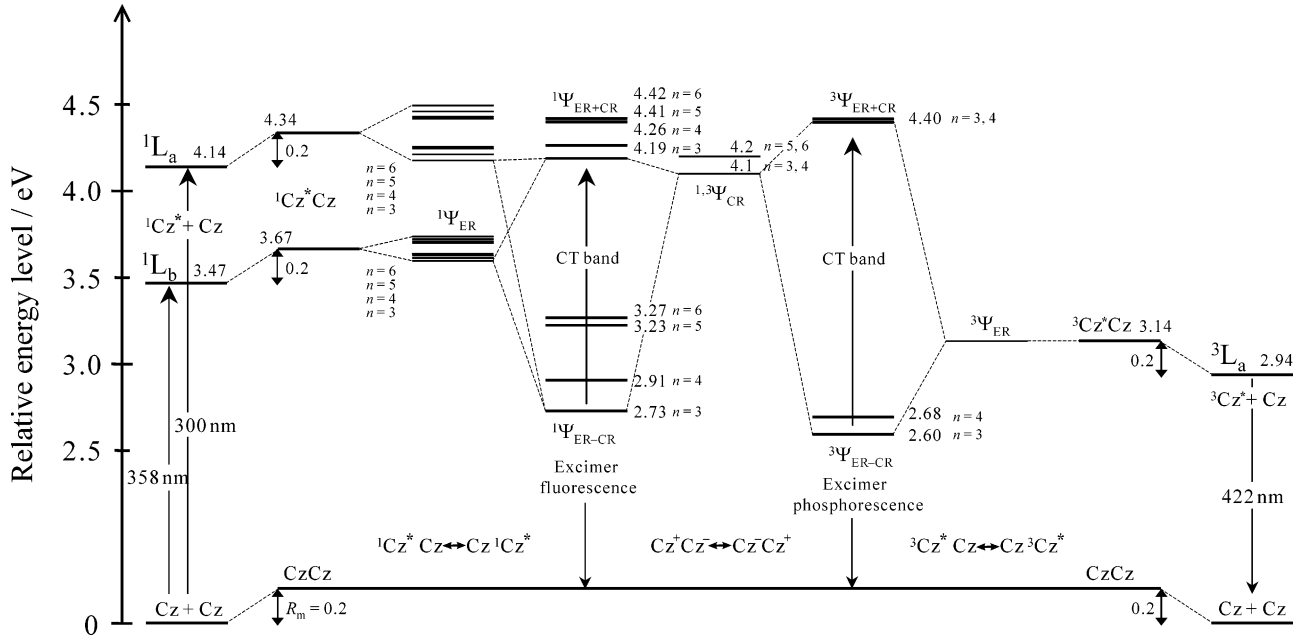

Figure 9. The schematic energy diagram for carbazole excimers formed in the singlet and triplet state. Energy in each state was determined on the basis of our spectroscopic data. The relative energy of a pair of carbazole molecules in the dimer configuration was assumed to be destabilized by 0.2 eV owing to the repulsive interaction. Details are described in the text.

Parameters used in the evaluation of E(CR) are $IP_g = 7.8$ eV,[20] $EA_g = 0$ eV,[20] $\epsilon = 7.52$,[77] $R = 3.75$ Å, and the average separation distance between two carbazole rings in [3.3.n]Cz was used as the separation distance between ions, r, in eq 2. This gives E(CR) = 4.1 eV for [3.3.n]Cz ($n = 3$, 4) and 4.2 eV for [3.3.n]Cz ($n = 5$, 6). In this figure, the energy levels of the monomer ^1L_b and ^1L_a states were evaluated from the absorption peaks at 300 and 358 nm of DMeCz observed in THF at 294 K. The energy level of the monomer ^3L_a state was evaluated from the 0−0 band of the DMeCz phosphorescence at 422 nm observed in MTHF at 130 K. The energy level of $^1\Psi_{ER-CR}$ and $^3\Psi_{ER-CR}$ states in each [3.3.n]Cz molecule was calculated by adding R_m (0.2 eV) to the energy of the peak wavelength of each fluorescence and phosphorescence band observed in MTHF at 130 K (Table 1). Similarly, the energy level of $^1\Psi_{ER+CR}$ and $^3\Psi_{ER+CR}$ states was calculated by addition of the transition energy in each CT band observed in THF at 294 K (Table 2) to the corresponding energy level of $^1\Psi_{ER-CR}$ and $^3\Psi_{ER-CR}$ states. This energy scheme can explain the increase in the transition energy (blue-shift) of the CT band in terms of the stabilization in the excimer fluorescence state in the order of [3.3.6]Cz < [3.3.5]Cz < [3.3.4]Cz < [3.3.3]Cz as shown in Figure 9.

In our previous report,[66] we simply discussed the excimer fluorescence of the [3.3.n]Cz molecules in terms of the ER interaction on the basis of the energy diagram proposed by Johnson, where the fluorescent excimer state is assigned to the lower ER state resulting from the exciton splitting of ^1L_a monomer state.[20] Here, we carefully reconsider the stabilization energy of excimer formation in the [3.3.n]Cz molecules. Figure 10a shows the stabilization energy caused by the ER interaction calculated on the basis of dipole−dipole approximation[78,79] for the monomer ^1L_b state (shaded bars)[80] and the experimental energy shift of the excimer fluorescence state from the corresponding ^1L_b state in the dimer configuration of 3.67 eV (closed bars). The stabilization of the ^1L_b state estimated from the ER interaction is substantially smaller than the fluorescence energy shift because the transition dipole moment is not so large. The stabilization energy due to the ER interaction is only 7.2% ($n = 3$), 7.0% ($n = 4$), 9.6% ($n = 5$), and 11% ($n = 6$) of the

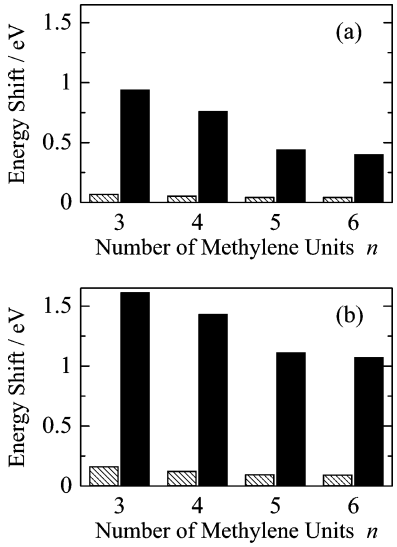

Figure 10. The stabilization energy of the singlet excimer formed in [3.3.n]Cz: the closed bars represent the observed energy shift of the excimer fluorescence state in each [3.3.n]Cz from the corresponding monomer (a) ^1L_b and (b) ^1L_a states in the dimer configuration; the shaded bars represent ER interaction of (a) ^1L_b and (b) ^1L_a states, which were calculated by using geometrical parameters r and θ for each state.[80,81] The energy of the monomeric ^1L_a and ^1L_b states in the dimer configuration was determined by adding the repulsion energy R_m = 0.2 eV to the energy of $^1L_b = 3.47$ eV and $^1L_a = 4.14$ eV, respectively.

fluorescence energy shift. As shown in Figure 10b, the same is true for the ^1L_a state: the stabilization due to the ER interaction (shaded bars)[81] is still too small to explain the observed large energy shift of the excimer fluorescence state from the corresponding ^1L_a state in the dimer configuration of 4.34 eV (closed bars). That is only 9.9% ($n = 3$), 8.6% ($n = 4$), 8.4% ($n = 5$), and 8.6% ($n = 6$) of the fluorescence energy shift. This large deviation indicates that the origin of the stabilization energy in [3.3.n]Cz singlet excimer is not merely the ER interaction but also the effective configurational mixing with the CR state, though we cannot assign which ER state contributes to the

excimer fluorescence state leading to the large stabilization by the configurational mixing.

Intermoiety Interaction in the Excited Triplet State. As shown in Figures 3 and 4, the broadening and the red-shift in the phosphorescence spectra of [3.3.*n*]Cz ($n = 3, 4, 5, 6$) provide evidence for intramolecular interaction between the two carbazole moieties in the phosphorescence state. In particular, the distinctly red-shifted and broad phosphorescence band observed for the [3.3.*n*]Cz ($n = 3, 4$) molecules can be safely assigned to the triplet excimer not only in solution at 130 K but also in rigid glass at 77 K. On the other hand, some monomeric vibrational bands still remained in the phosphorescence spectra of [3.3.*n*]Cz ($n = 5, 6$), indicating that the intramolecular interaction is insufficient to induce excimeric phosphorescence in the rigid glass at 77 K and also in solution at 130 K. Similar to that of the carbazole singlet excimer, this tendency suggests that $r \sim 4$ Å is a critical distance to form a carbazole triplet excimer, and the parallel configuration is more favorable for the triplet excimer than the largely inclined configuration. Thus, we conclude that the stable conformation for the carbazole triplet excimer is essentially the same as the singlet one. This conclusion is different from that proposed for naphthalene excimers.[43−45] The naphthalene singlet excimer is in a sandwich configuration while the triplet excimer is in an L-shape configuration. Note the difference between the fluorescence and the phosphorescence of [3.3.5]Cz at 130 K: the former is an excimer-like emission and the latter is a monomer-like one. The difference suggests that the conformation to form the triplet excimer is limited more strictly compared to that of the singlet excimer, an issue we will discuss in more detail in the next section.

In contrast to singlet excimers, the stabilization due to the ER interaction is generally negligible in triplet excimers because of a spin-forbidden transition. Thus, the phosphorescence state cannot be stabilized by the ER interaction; the energy level of the lowest ER state is almost the same as that of the locally excited triplet states T_1. Therefore, the configurational mixing between the ER and CR states plays an essential role in the formation of triplet excimers. As discussed in the previous subsection, the contribution of the configurational mixing can be evaluated from the transient absorption spectra in accordance with the energy scheme shown in Figure 9. Thus, our observation of the CT band in the $T_n \leftarrow T_1$ absorption spectra reveals the existence of the effective configurational mixing in the triplet state for all carbazolophanes at 294 K. Therefore, we conclude that a carbazole triplet excimer can be formed at 294 K, although no phosphorescence was observed. The lack of phosphorescence may be attributed to enhancement of the nonradiative deactivation at the higher temperature. Furthermore, the CT band in the triplet state was blue-shifted in the order of [3.3.6]Cz $\approx$ [3.3.5]Cz < [3.3.4]Cz < [3.3.3]Cz, indicating that the phosphorescence excimer state is also stabilized by the configurational mixing in the same order as in the case of the singlet excimer. This agreement is consistent with our conclusion that carbazole excimers are stable in the parallel-sandwich configuration whether in the singlet or triplet states.

Comparison between Singlet and Triplet Carbazole Excimers. As discussed above, both singlet and triplet excimers of carbazole are primarily stabilized by the configurational mixing between the ER and CR states. This interaction is generally called the CT interaction that requires effective orbital overlap between the two chromophores. The importance of large orbital overlap in the excimer formation is consistent with our previous study on *syn*- and *anti*-[3.3](3,9)carbazolophanes[63] as model compounds for fully and partially overlapped excimers, respectively. Furthermore, theoretical calculations also indicate that a larger orbital overlap makes the excimer state more stable whether in the singlet state or in the triplet state.[2,7,9] However, we should note that the formation of the carbazole triplet excimer is more restricted compared with the singlet excimer. The difference can be clearly seen in the total emission spectrum of [3.3.5]Cz in PBMA film at 77 K. As mentioned before, the [3.3.5]Cz molecule exhibited broad excimer fluorescence but monomer-like structured phosphorescence as shown in Figure 5. This clear difference suggests that the driving force for the carbazole excimer formation is larger in the singlet state than in the triplet state. Theoretically, the stabilization due to the configurational mixing is inversely proportional to the square of the energy gap between the interacting ER and CR states.[4] The energy difference from the CR state is evaluated to be ~1 eV for the ^3L_a state, ~0.5 eV for the lower ER state from ^1L_b, and ~0.1 eV for the lower ER state from ^1L_a. The larger energy difference would provide less stabilization to the configurational mixing in the triplet state (^3L_a) than in the singlet state (^1L_b or ^1L_a) even in the same dimer configuration. We therefore conclude that no triplet excimer formation at 130 K in [3.3.5]-Cz or [3.3.6]Cz results from the large energy difference between the triplet ER and CR states, which might not cause attractive force in the two carbazole rings enough to induce larger orbital overlapping leading to excimer formation.

Note that the energy gap between the singlet excimer state and the triplet excimer state for each [3.3.*n*]Cz molecule systematically decreases with decreasing *n*. This dependence is fully consistent with our conclusion that the carbazole singlet excimer is more stabilized than the triplet one because of not only the contribution of the ER interaction but also the larger configurational mixing owing to proper energy matching between the ER and CR states. Furthermore, the energy gap ΔE_{ST} is closely related to the electron exchange interaction $2J$ in the molecular system. In most aromatic molecules, the lowest excited triplet state is more stable by $2J$ than the lowest excited singlet state. For DMeCz monomer, ΔE_{ST} was estimated to be 0.53 eV, which is smaller than aromatic hydrocarbons ($\Delta E_{ST} > 1$ eV)[82] but comparable to aromatic amines, such as diphenyl amine, iminobibenzyl, acridan, and carbazole.[83] For carbazolophane excimers, ΔE_{ST} is as small as 0.13 eV for [3.3.3]Cz and 0.23 eV for [3.3.4]Cz, which are 0.3−0.4 eV smaller than that for DMeCz. A similar decrease in ΔE_{ST} is seen in aromatic hydrocarbons. For example, ΔE_{ST} of anthracene decreases by 0.2 eV compared to that of naphthalene and by 0.4 eV compared to that of benzene,[82] indicating that the ΔE_{ST} values are smaller in larger aromatic molecules. Therefore, the small ΔE_{ST} value suggests that the electrons are effectively delocalized over the two carbazole moieties in the excimer states. EPR measurements have revealed that charge delocalization occurs in the carbazole excimer state.[68] The effective electron delocalization is consistent with the larger configurational mixing between the ER and CR states when *n* is small.

Conclusions

We studied the intermoiety electronic interactions in the singlet and triplet excimer states using triply bridged [3.3.*n*]-(3,6,9)carbazolophanes ([3.3.*n*]Cz, $n = 3, 4, 5, 6$), where the dihedral angle θ and the average separation distance *r* between the two carbazole moieties change systematically from almost parallel ($n = 3$; $\theta = 2.6°$, $r = 3.35$ Å) to oblique ($n = 6$; $\theta = 33.1°$, $r = 4.03$ Å) with the increase in the number of methylene units *n* bridging at 9-position of each carbazole ring. On the

basis of well-defined structures of our carbazolophanes, we arrived at several important findings on the intermoiety interaction in singlet and triplet excimers of carbazole. First, only [3.3.*n*]Cz ($n = 3, 4$, $r < 4$ Å) exhibited excimer fluorescence and phosphorescence in rigid glass at 77 K where these molecules would be in the most stable conformation as revealed by X-ray analysis, suggesting that both singlet and triplet excimers of carbazole are formed with a separation distance shorter than about 4 Å. This critical distance is consistent with previous theoretical calculations for aromatic hydrocarbons. Second, [3.3.3]Cz exhibited the most red-shifted excimer emissions in not only fluorescence but also phosphorescence, suggesting that the most stable conformation is the parallel-sandwich structure rather than inclined configuration for not only singlet but also triplet excimers of carbazole. This is different from naphthalene excimers for which the L-shape configuration is considered to be one of the preferred geometries in their triplet state. Third, [3.3.5]Cz exhibited excimer fluorescence but monomer-like vibrational phosphorescence in a PBMA glassy film at 77 K, suggesting limited formation of the carbazole triplet excimer compared to the carbazole singlet excimer. This is partly because of the lack of the ER interaction in the triplet state but mainly because of the larger energy gap between the ER and CR states in the triplet state resulting in lower stabilization than in the singlet state. Fourth, the transient absorption spectra measured at 294 K exhibited CT bands for all [3.3.*n*]Cz molecules in the excited singlet and triplet states, suggesting that the configurational mixing contributes to the formation of carbazole excimers and that not only singlet but also triplet carbazole excimers can be formed in liquid solution at 294 K, although no phosphorescence was observed. The stabilization of the carbazole singlet excimer appeared to originate partly from the ER interaction, as we discussed previously, but mainly from the configurational mixing between the ER and the CR states. Finally, the singlet−triplet energy gap was found to decrease with decreasing *n*, suggesting effective electron delocalization over the two carbazole rings, consistent with the larger configurational mixing when *n* is small.

Acknowledgment. This work was partly supported by a Grant-in-Aid for Young Scientist (B) (No. 16750187) from the Ministry of Education, Culture, Sports, Science and Technology of Japan.

References and Notes

(1) Förster, T.; Kasper, K. *Z. Elektrochem.* **1955**, *59*, 976−980.
(2) McGlynn, S. P.; Armstrong, A. T.; Azumi, T. In *Modern Quantum Chemistry, Part III*; Sinanoğlu, O., Ed.; Academic Press: New York, 1965; pp 203−228.
(3) Birks, J. B. *Photophysics of Aromatic Molecules*; Wiley-Interscience: London, 1970; pp 301−371.
(4) Birks, J. B. *Rep. Prog. Phys*. **1975**, *38*, 903−974.
(5) Barashkov, N. N.; Sakhno, T. V.; Nurmukhametov, R. N.; Khakhel', O. A. *Russ. Chem. Rev.* **1993**, *62*, 539−552.
(6) Konijnenberg, E. Doctoral Thesis, University of Amsterdam, 1963.
(7) Murrell, J. N.; Tanaka, J. *Mol. Phys.* **1964**, *7*, 363−380.
(8) Azumi, T.; McGlynn, S. P. *J. Chem. Phys.* **1964**, *41*, 3131−3138.
(9) Azumi, T.; Armstrong, A. T.; McGlynn, S. P. *J. Chem. Phys.* **1964**, *41*, 3839−3852.
(10) Hirayama, F. *J. Chem. Phys.* **1965**, *42*, 3163−3171.
(11) Chandross, E. A.; Dempster, C. J. *J. Am. Chem. Soc.* **1970**, *92*, 3586−3593.
(12) Ito, S.; Yamamoto, M.; Nishijima, Y. *Bull. Chem. Soc. Jpn.* **1981**, *54*, 35−40.
(13) Ito, S.; Yamamoto, M.; Nishijima, Y. *Bull. Chem. Soc. Jpn.* **1982**, *55*, 363−368.
(14) Klöpffer, W. *Chem. Phys. Lett.* **1969**, *4*, 193−194.
(15) Klöpffer, W. *J. Chem. Phys.* **1969**, *50*, 2337−2343.
(16) Zachariasse, K.; Kühnle, W. *Z. Phys. Chem.* **1976**, *101*, 267−276.
(17) Yamamoto, M.; Goshiki, K.; Kanaya, T.; Nishijima, Y. *Chem. Phys. Lett.* **1978**, *56*, 333−336.
(18) Kanaya, T.; Goshiki, K.; Yamamoto, M.; Nishijima, Y. *J. Am. Chem. Soc.* **1982**, *104*, 3580−3587.
(19) Semerak, S. N.; Frank, C. W. *Adv. Polym. Sci.* **1984**, *54*, 31−85.
(20) Johnson, G. E. *J. Chem. Phys.* **1975**, *62*, 4697−4709.
(21) Itaya, A.; Okamoto, K.; Kusabayashi, S. *Bull. Chem. Soc. Jpn.* **1976**, *49*, 2082−2088.
(22) De Schryver, F. C.; Vandendriessche, J.; Toppet, S.; Demeyer, K.; Boens, N. *Macromolecules* **1982**, *15*, 406−408.
(23) Vandendriessche, J.; Palmans, P.; Toppet, S.; Boens, N.; De Schryver, F. C.; Masuhara, H. *J. Am. Chem. Soc.* **1984**, *106*, 8057−8064.
(24) Collart, P.; Toppet, S.; Zhou, Q. F.; Boens, N.; De Schryver, F. C. *Macromolecules* **1985**, *18*, 1026−1030.
(25) De Schryver, F. C.; Collart, P.; Vandendriessche, J.; Goedeweeck, R.; Swinnen, A.; Van der Auweraer, M. *Acc. Chem. Res.* **1987**, *20*, 159−166.
(26) Evers, F.; Kobs, K.; Memming, R.; Terrell, D. R. *J. Am. Chem. Soc.* **1983**, *105*, 5988−5995.
(27) Ito, S.; Takami, K.; Tsujii, Y.; Yamamoto, M. *Makromol. Chem., Rapid Commun.* **1989**, *10*, 79−84.
(28) Ito, S.; Takami, K.; Tsujii, Y.; Yamamoto, M. *Macromolecules* **1990**, *23*, 2666−2673.
(29) Yokoyama, M.; Funaki, M.; Mikawa, H. *J. Chem. Soc., Chem. Commun.* **1974**, 372−373.
(30) Burkhart, R. D.; Avilés, R. G. *J. Phys. Chem.* **1979**, *83*, 1897−1901.
(31) Burkhart, R. D.; Dawood, I. *Macromolecules* **1986**, *19*, 447−452.
(32) Starzyk, F. C.; Burkhart, R. D. *Macromolecules* **1989**, *22*, 782−786.
(33) Burkhart, R. D.; Chakraborty, D. K. *J. Phys. Chem.* **1990**, *94*, 4143−4147.
(34) Burkhart, R. D.; Jhon, N. I.; Boileau, S. *Macromolecules* **1991**, *24*, 6310−6317.
(35) Ito, S.; Katayama, H.; Yamamoto M. *Macromolecules* **1988**, *21*, 2456−2462.
(36) Katayama, H.; Hisada, K.; Yanagida, M.; Ohmori, S.; Ito, S.; Yamamoto, M. *Thin Solid Films* **1992**, *224*, 253−256.
(37) Wada, Y.; Ito, S.; Yamamoto, M. *J. Phys. Chem.* **1993**, *97*, 11164−11167.
(38) Ito, S.; Yamamoto, M.; Liebe, W. R.; Burkhart, R. D.; Wada, Y. *J. Phys. Chem.* **1994**, *98*, 7608−7612.
(39) Kim, N.; Webber, S. E. *Macromolecules* **1980**, *13*, 1233−1236.
(40) Burkhart, R. D.; Avilés R. G.; Magrini, K. *Macromolecules* **1981**, *14*, 91−95.
(41) Zachariasse, K. A.; Busse, R.; Schrader, U.; Kühnle, W. *Chem. Phys. Lett.* **1982**, *89*, 303−308.
(42) Tamai, N.; Masuhara, H.; Mataga, N. *J. Phys. Chem.* **1983**, *87*, 4461−4467.
(43) Lim, E. C. *Acc. Chem. Res.* **1987**, *20*, 8−17.
(44) East, A. L. L.; Lim, E. C. *J. Chem. Phys.* **2000**, *113*, 8981−8994.
(45) Terazima, M.; Cai, J.; Lim. E. C. *J. Phys. Chem. A* **2000**, *104*, 1662−1669.
(46) Cram, D. J.; Allinger, N. L.; Steinberg, H. *J. Am. Chem. Soc.* **1954**, *76*, 6132−6141.
(47) Froines, J. R.; Hagerman, P. J. *Chem. Phys. Lett.* **1969**, *4*, 135−138.
(48) Cram, D. J.; Cram, J. M. *Acc. Chem. Res.* **1971**, *4*, 204−213.
(49) Schweitzer, D.; Colpa, J. P.; Behnke, J.; Hausser, K. H.; Haenel, M.; Staab, H. A. *Chem. Phys.* **1975**, *11*, 373−384.
(50) Hayashi, T.; Mataga, N.; Umemoto, T.; Sakata, Y.; Misumi, S. *J. Phys. Chem.* **1977**, *81*, 424−429.
(51) Morita, M.; Kishi, T.; Tanaka, M.; Tanaka, J.; Ferguson, J.; Sakata, Y.; Misumi, S.; Hayashi, T.; Mataga, N. *Bull. Chem. Soc. Jpn.* **1978**, *51*, 3449−3457.
(52) Ishikawa, S.; Nakamura, J.; Iwata, S.; Sumitani, M.; Nagakura, S.; Sakata, Y.; Misumi, S. *Bull. Chem. Soc. Jpn.* **1979**, *52*, 1346−1350.
(53) Otsubo, T.; Kitasawa, M.; Misumi, S. *Bull. Chem. Soc. Jpn.* **1979**, *52*, 1515−1520.
(54) Blank, N. E.; Haenel, M. W. *Chem. Ber.* **1981**, *114*, 1520−1530.
(55) Blank, N. E.; Haenel, M. W. *Chem. Ber.* **1981**, *114*, 1531−1538.
(56) Ferguson, J. *Chem. Rev.* **1986**, *86*, 957−982.
(57) Yanagidate, M.; Takayama, K.; Takeuchi, M.; Nishimura, J.; Shizuka, H. *J. Phys. Chem.* **1993**, *97*, 8881−8888.
(58) Nakamura, Y.; Tsuihiji, T.; Mita, T.; Minowa, T.; Tobita, S.; Shizuka, H.; Nishimura, J. *J. Am. Chem. Soc.* **1996**, *118*, 1006−1012.
(59) Nishimura, J.; Nakamura, Y.; Hayashida, Y.; Kudo, T. *Acc. Chem. Res.* **2000**, *33*, 679−686.
(60) Nakamura, Y.; Fujii, T.; Nishimura, J. *Tetrahedron Lett.* **2000**, *41*, 1419−1423.
(61) Yamaji, M.; Tsukada, H.; Nishimura, J.; Shizuka, H.; Tobita, S. *Chem. Phys. Lett.* **2002**, *357*, 137−142.

(62) Nogita, R.; Matohara, K.; Yamaji, M.; Oda, T.; Sakamoto, Y.; Kumagai, T.; Lim, C.; Yasutake, M.; Shimo, T.; Jefford, C. W.; Shinmyozu, T. *J. Am. Chem. Soc.* **2004**, *126*, 13732−13741.

(63) Tani, K.; Tohda, Y.; Takemura, H.; Ohkita, H.; Ito, S.; Yamamoto, M. *Chem. Commun.* **2001**, 1914−1915.

(64) Nakamura, Y.; Kaneko, M.; Tani, K.; Shinmyozu, T.; Nishimura, J. *J. Org. Chem.* **2002**, *67*, 8706−8709.

(65) Ohkita, H.; Ito, S.; Yamamoto, M.; Tohda, Y.; Tani, K. *J. Phys. Chem. A* **2002**, *106*, 2140−2145.

(66) Benten, H.; Ohkita, H.; Ito, S.; Yamamoto, M.; Sakumoto, N.; Hori, K.; Tohda, Y.; Tani, K.; Nakamura Y.; Nishimura, J. *J. Phys. Chem. B* **2005**, *109*, 19681−19687.

(67) Tani, K.; Sakumoto, N.; Kubono, K.; Hori, K.; Tohda, Y.; Benten, H.; Ohkita, H.; Ito, S.; Yamamoto, M. *Chem. Commun.,* to be submitted for publication.

(68) Saiful, I. S. M.; Heinze, P.; Ohba, Y.; Yamauchi, S.; Yamamoto, M.; Tohda, Y.; Tani, K. *Mol. Phys.* **2006**, *104*, 1535−1542.

(69) Masuhara, H.; Tamai, N.; Mataga, N.; De Schryver, F. C.; Vandendriessche, J. *J. Am. Chem. Soc.* **1983**, *105*, 7256−7262.

(70) Yamamoto, M.; Tsujii, Y.; Tsuchida A. *Chem. Phys. Lett.* **1989**, *154*, 559−562.

(71) Kikuchi, K. *Triplet−Triplet Absorption Spectra*; Bunshin Publishing Company: Tokyo, 1989; p 107.

(72) Katoh, R.; Katoh, E.; Nakashima, N.; Yuuki, M.; Kotani, M. *J. Phys. Chem. A* **1997**, *101*, 7725−7728.

(73) Sadygov, R. G.; Lim, E. C. *Chem. Phys. Lett.* **1994**, *225*, 441−447.

(74) Born, M. *Z. Phys.* **1920**, *1*, 45−48.

(75) Edward, J. T. *J. Chem. Educ.* **1970**, *47*, 261−270.

(76) Katoh, R.; Lacmann, K.; Schmidt, W. F. *Z. Phys. Chem.* **1995**, *190*, 193−201.

(77) *CRC Handbook of Chemistry and Physics*, 87th ed.; CRC Press: Boca Raton, 2006; p 8-128.

(78) Kasha, M. *Radiat. Res.* **1963**, *20*, 55−70.

(79) McRae, E. G.; Kasha, M. In *Physical Process in Radiation Biology*; Augenstein, L., Mason, R., Rosenberg, B., Eds.; Academic Press: New York, 1964; pp 23−42.

(80) The exciton splitting energy ΔE for monomer ^1L_b state was calculated assuming that α and β are equal to $(180° - \theta)/2$ in the equation $\Delta E = 2|\boldsymbol{M}|^2(\cos\theta + 3\cos\alpha\cos\beta)/r^3$, where $\boldsymbol{M}$ is the transition dipole moment from the ground ^1A to the ^1L_b state and r and θ are the average separation distance and the dihedral angle formed between two carbazole rings, respectively.[66] The value of $\boldsymbol{M}$ was evaluated to be ca. 2.0×10^{-18} esu cm (2.0 D) by using the equation $\tau_f^0 = 3hc^3/(64\pi^4\nu^3|\boldsymbol{M}|^2)$, where τ_f^0 is the natural fluorescence lifetime of DMeCz in MTHF at 294 K ($\tau_f^0 = 3.6 \times 10^{-8}$ s), ν the frequency for the absorption maximum of the ^1L_b band at 358 nm ($\nu = 8.4 \times 10^{-8}$ s^{-1}), h the Planck's constant, and c the velocity of light. The shaded bars in Figure 10a show $\Delta E/2$.

(81) The exciton splitting energy ΔE for monomer ^1L_a state was calculated by using the equation $\Delta E = 2|\boldsymbol{M}|^2/r^3$, where $\boldsymbol{M}$ is the transition dipole moment from the ground ^1A to the ^1L_a state and r is the average separation distance between the two carbazole rings. The value of $\boldsymbol{M}$ was evaluated to be ca. 3.1×10^{-18} esu cm (3.1 D) by using the equation $f = 4.703 \times 10^{29}\,\tilde{\nu}|\boldsymbol{M}|^2$, where f is the oscillator strength for the $^1L_a \leftarrow {}^1A$ transition ($f = 0.15$) and $\tilde{\nu}$ is the frequency at the absorption maximum 300 nm of the ^1L_a band ($\tilde{\nu} = 33\,300$ cm^{-1}). The value of f was calculated by integrating the molar extinction coefficient ϵ of DMeCz in THF at 294 K over the $^1L_a \leftarrow {}^1A$ absorption region. The shaded bars in Figure 10b show $\Delta E/2$.

(82) Turro, N. J. *Modern Molecular Photochemistry*; The Benjamin/Cummings Publishing Co.: California, 1978; p 31.

(83) Adams, J. E.; Mantulin, W. W.; Huber, J. R. *J. Am. Chem. Soc.* **1973**, *95*, 5477−5481.